PART-IV
Quantum Optics

12 Degenerate Four-Wave Mixing in DASPB Dye-Doped Polymer Film

S. Aithal, P. S. Aithal and N.G. Bhat

12.1 Introduction

Non-linear optical phase conjugation by degenerate four-wave mixing (DFWM) is an important technique with applications in many fields of science and technology including image transmission, optical image processing, optical filtering, and laser resonators[14, 29, 8]. When two counter-propagating and intense light beams interact with a non-linear medium, together with a less intense third one, a fourth beam is generated from the medium, which will be the phase conjugation of the third beam. This technique is called four-wave mixing. The unique feature of a pair of phase conjugate beams is that the aberration influence imposed on the forward (signal) beam passed through an inhomogeneous or disturbing medium can be automatically removed from the backward (phase conjugated) beam passed through the same disturbing medium[11]. The main applications of degenerate DFWM techniques are non-linear spectroscopy, real time holography, and phase conjugation. Phase conjugation by DFWM has been demonstrated in many organic and inorganic materials using pulsed or continuous-wave (CW) lasers[27, 12].

The phase conjugate light has a variety of characteristics and properties not associated with normal light and they can be enumerated as follows:

(1) *Phase compenzation effect:* Waves that pass through an aberrating medium are injected into a phase conjugate mirror. If the outgoing wave is re-propagated through the medium, the waves phase distortion is compensated.

(2) *Space domain multiplicative interaction:* Since phase conjugate waves are produced by interaction in a non-linear medium, the spatial multiplicative effect among the light waves appears in the phase conjugate waves.

(3) *Intensity dependant phase shift:* Due to the optical Kerr effect in a non-linear medium, the phase shift of the electric field depends on the wave intensity.

(4) *Detuning dependence:* The reflectance of a phase conjugate mirror strongly depends on the detuning between the pump and probe wave frequencies.

(5) *Time inversion:* A phase conjugate wave can be regarded as a time inverted wave since its direction of propagation is exactly opposite that of the probe wave and the wave front is identical to that of the probe wave.

(6) *Time domain multiplicative interaction:* When pulsed waves are used in the production of phase conjugate light, the resulting polarization, that is, the generalized phase conjugate wave intensity depends on the product of the interacting waves in the waves' temporal domains.

(7) *Quantum correlation:* When waves are treated quantum theoretically, the probe and phase conjugate waves correspond the photon annihilation and creation operators respectively.

Organic molecules exhibit large polarizabilities because exited π-bond electrons are delocalized and hence easily polarizable[19]. Saturable absorption plays a very important role when dyes are used for the production of phase conjugation light, because χ^3 is inversely proportional to the saturation intensity[16]. These systems exhibit large third-order susceptibilities. OPC has been reported in glasses and other solid matrices doped by organic dyes emerging as promising materials for OPC because of their large third-order non-linear susceptibilities $\chi^{(3)}$. In these materials, the phase conjugate wave can be generated at low light intensities provided by the continuous wave lasers. Moreover, these materials can be easily prepared in the laboratories.

Figure 12.1 shows the energy level diagram of dyes. These materials can be explained by a three-level system[24]. When light is injected, electrons excite from the S_0 level to the S_1 level. The dye molecules will switch over to the triplet state. The number of electrons at the S_0 level is reduced only by the number of electrons occupying the T_1 level. Therefore, the number of excitable electrons at the S_0 level is dramatically reduced if the intensity of the injected waves is high at a frequency corresponding to the S_0 and S_1 levels energy; the rate of absorption is thus reduced[8]. Thus, absorption becomes a function of intensity. The gratings produced by interference between the probe and pump wave are such that the period can be determined using the following relation :

$$\Lambda = \frac{2n}{K_G} = \frac{\lambda}{2n\sin\theta/2}, \tag{12.1}$$

where λ is the laser wavelength. At a small angle θ, the spacing is wider for a transmission grating than for a reflection grating[6, 5]. The theory of DFWM was formulated for a two-level saturable absorber by Abraham and Lind[1] and was modified to describe a three-level absorber (Fig. 12.1) by Silberberg and Bar-Joseph[25]. The phase conjugated reflectivity is then given by

$$R = \frac{|k|^2}{[a + w\cot(wL)]^2}, \tag{12.2}$$

where $w = (|k|^2 - a^2)^{\frac{1}{2}}$ and a is the saturated absorption co-efficient given by

$$a = a_0 \frac{1 + I_1 + I_2}{[1 + 2(I_1 + I_2) + (I_1 - I_2)^2]^{3/2}} \tag{12.3}$$

and the coupling coefficient k is given by

$$k^* = 2a_0 i \frac{(I_1.I_2)}{[1 + 2(I_1 + I_2) + (I_1 - I_2)^2]^{3/2}}. \tag{12.4}$$

I_1 and I_2 are two pump beam intensities normalized by the saturation intensity I_s[25].

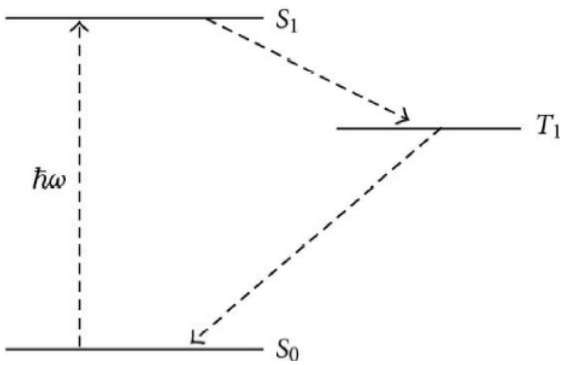

Figure 12.1 Energy level diagram of a three-level model for organic dyes

12.2 Non-linear Processes

Non-linear processes like non-linear refraction, thermal grating, saturation and reverse saturation absorption, two photon induced fluorescence, photorefraction, and stimulated Brillouin scattering lead to the formation of a laser-induced grating in the medium are associated with the generation of phase conjugated wave.

12.2.1 Non-linear refraction

In non-linear refraction, the refractive index of the material varies with light intensity. Materials with positive non-linear refractive index shows self-focusing and materials with negative non-linear refractive index gives rise to self-defocusing. For a purely third order response with input irradiance I_0,

$$\Delta n = n_2 I_0, \tag{12.5}$$

where n_2 is non-linear refractive index and is positive for self-focusing materials and is negative for self-defocusing materials. The non-linear optical properties of materials range from the index change due to the ultrafast interaction of light with bound electrons to the index change caused by the relatively slow thermal expansion of a liquid due to linear absorption. The effects caused by these non-linear interactions with matter range from the reduction of transmittance from increasing absorption with increasing irradiance (e.g., two-photon absorption) to beam spreading from self-defocusing to the ultimate non-linear interaction of laser-induced damage.

12.2.2 Thermal gratings

Thermal effect of illuminated light beam may create large non-linear optical effects and hence the temperature of the illuminated portion of the material increases; the refractive index invariably decreases with increasing temperature[4]. This intensity-dependent change of the refractive index in liquids or solids may result in very significant self-diffraction effects for phase conjugate beam generation. From early works on these mechanisms, it is well established from heat equations that the steady-state index modulation varies as the square of the grating period and is inversely proportional to the thermal conductivity of the material. Therefore, for small grating periods, thermal diffusion tends to reduce both the photoinduced index modulation amplitude and the diffraction efficiency of thermal holograms. For that reason, wave-mixing experiments based on thermal non-linearities will benefit from using a small pump-probe beam angle or a longer wavelength up to 10 μm.

Under steady-state conditions, the heat transport equation reduces to

$$\frac{\Delta(nL)}{nL} = \frac{1}{n}\frac{\partial n}{\partial T}\Delta T + \frac{1}{L}\frac{\partial L}{\partial L}\Delta T, \tag{12.6}$$

where n is refractive index and L is sample thickness[18, 5]. To perform efficient wave mixing, phase conjugation materials that display high thermal coefficient must be used, and this condition can be achieved in semiconductors like HgCdTe where $\partial n/\partial T$ is 10^{-3} at $\lambda = 10.6$ μm, or in liquid crystals where $\partial n/\partial T = 10^{-3}$ at room temperature and $\partial n/\partial T = 10^{-2}$ near the transition temperature[15].

12.2.3 Saturation and reverse saturation absorption

Saturable absorption was recognized early as an efficient mechanism for efficient phase conjugation. It is based on the dependence of the absorption and refractive index of two-level or three-level systems on the incident average intensity due to pump and probe beams. It is expected that transitions with a large cross-section and a long relaxation time are more easily saturable. The basic absorption processes in dyes can be divided into linear and non-linear absorption. Non-linear absorption is a phenomenon defined as a non-linear change (increase or decrease) in absorption with increasing intensity. This can be of either two types: saturable absorption (SA) and reverse saturable absorption (RSA). Depending on the pump intensity and on the absorption cross-section at the excitation wavelength, most molecules show non-linear absorption. With increasing intensity, if the excited states show saturation owing to their long life times, the transmission will show SA characteristics. If, however, the excited state has strong absorption compared with that of the ground state, the transmission will show RSA characteristics. These absorption characteristics are highly dependent on the wavelength, intensity and excited state lifetime. With the availability of intense laser sources, it is essential to have perfect knowledge of the absorption characteristics of the medium. SA is vital for use of dyes in mode locking. The most important application of RSA is in an optical limiting device[25] that protects sensitive optical components, including the human eye, from laser-induced damage. RSA is observed as a result of excited state absorption (ESA), TPA, or both.

Non-linear absorption parameters were therefore calculated for an effective three-level system with S_0, S_1, and S_n states. For the saturation of a homogeneously broadened line, the dependence of measured absorption coefficient α on intensity I of the incident laser radiation is given by the expression[23]

$$\alpha = \frac{\alpha_0}{1} + \frac{I}{I_s}, \tag{12.7}$$

where α_0 is the low-intensity absorption coefficient and I_S is the saturation intensity.

A strong, narrow band laser field saturates one segment of the inhomogeneous absorption profile (e.g., Doppler broadening), leading to decreased absorption. Malcuit et al.[17] proposed the following equation for this kind of inhomogeneous saturation:

$$\alpha = \frac{\alpha_0}{1 + (I/I_s)^{1/2}}. \tag{12.8}$$

Samoc et al.[22] observed SA in poly(indenofluorene), and they found that the experimental curves were not well reproduced by Eqs (12.7) and (12.8), proposed the following *ad hoc* formula, and obtained a satisfactory fit:

$$\alpha = \frac{\alpha_0}{1 + (I/I_s)^{1/2}}. \tag{12.9}$$

12.2.4 Two photon induced florescence

According to the basic theoretical consideration, the TPA induced decrease of transmissivity can be expressed as

$$I(L) = \frac{I_0}{(1 + I_0 L\beta)}, \tag{12.10}$$

where $I(L)$ is the transmitted beam intensity, I_0, is the incident beam intensity, L is the thickness of the sample, and β is the TPA coefficient of the sample medium. In the derivation of Eq. (12.10), it is assumed that the linear attenuation of the medium can be neglected and the beam has a nearly uniform transverse intensity distribution within the medium. Using Eq. (12.10), the value of β can be determined by measuring the transmitted intensity versus the incident intensity for a sample medium with a given L value. Furthermore, the TPA coefficient (in units of cm/GW) of a given sample is determined by

$$\beta = \sigma_2 N_o = \sigma_2 N_A d_o \times 10^{-3} \tag{12.11}$$

Here, N_o is the molecular density of the dopant (in units of 1 cm^3), σ_2 is the molecular TPA coefficient (or cross-section) of the same dopant (in units of cm^4/GW), d_o is the concentration of the dopant compound in the matrix (in units of M), and finally N_A is Avogadro's number. For known values of β and d_o, the value of σ_2 can be calculated from Eq. (12.11).

Non-linear absorption coefficient is also calculated for an effective three-level system with S_0, S_1, and S_n states by using the β value determined from the theoretical fits to calculate the TPA cross-section (σ_{TPA}) from the following relation[13]:

$$\beta = \frac{N_0}{h\vartheta}\sigma_{TPA}, \tag{12.12}$$

where h is Planck's constant, ϑ is the frequency of light, and N_0 is the number of molecules per unit volume.

12.2.5 Photorefraction

Photorefraction is a particular type of non-linearity which arises in materials that exhibit linear (or quadratic) electro-optic (EO) effects. The illumination of the material by a two-beam interference pattern generates a photoinduced charge distribution. The photogenerated carriers (electrons or holes) are trapped, and thus it results in a space charge field in the volume of the material which modulates the refractive index through the electro-optics coefficient. Microscopic phenomena for space charge buildup involves electrons charge diffusion or drift under an external applied electric field. There are several specific characteristics of the photorefractive effect which differ from other known non-linear mechanisms. First, there is no threshold effect and the material responds to the incident energy. In such conditions, the material response time can be easily controlled from a fraction of a microsecond to several seconds; second, the amplitude of the photoinduced index modulation is mainly determined by the value of the electro-optic coefficient and by the trapping center density. Moreover, photorefractive materials have a dark storage time constant, equivalent to memory effect[26, 7]. Photorefractive materials have already demonstrated their great importance in experiments based on the recording and erasure of holograms for optical information processing, high-gain wave mixing, and phase conjugation with low-power visible or near-infrared laser beams. Most of the experiments were performed with different types of EO materials such as $LiNbO_3$, $BaTiO_3$, and Bi_{12} (Si, Ge, Ti) O_{20}; semiconductors such as GaAs, InP, and CdTe; PLZT ceramics; and, more recently, doped EO polymers or liquid crystals[15].

12.2.6 Stimulated Brillouin scattering

The stimulated Brillouin scattering (SBS) effect originates from the electrostrictive effect in the transparent dielectric media such as liquids, gases or solids. The interference patterns due to the incident and spontaneous scattered optical fields generate a traveling acoustic wave that modulates the material refractive index through the elasto-optic effect. It thus results from the interaction, the equivalent of a coherent moving phase grating that propagates at sound velocity and that diffracts in the backward direction, a phase conjugate replica of the incident high intensity laser beam. SBS is a phenomenon that exhibits a threshold, and its typical response time ranges in the nanosecond due to the phonon lifetime. Moreover, because of the moving grating, the retro-reflected Stokes wave is frequency-shifted by the Doppler effect corresponding to the sound velocity by several gigahertz. SBS is a very well suited interaction for self-pumped phase conjugation and most efficient materials are high-pressure gases (SF_6, N_2, Xe, etc.), liquids (CS_2, CCl_4, $GeCl_4$, $SiCl_4$, $TiCl_4$, freon, acetone, etc.), or solids (silica fibers or bulk, quartz, organic crystals such as LAP, DLAP, etc.)[15].

In this chapter, PC wave generation in dye 4-[4-(Dimethylamino)styryl]-1- docosyl pyridinium bromide (DASPB) doped in PMMA-MA polymer matrix using low-power continuous wave laser excitation is presented. PC signal strength at different times for different dye doped concentration, PC reflectivity a function of angle between the probe beam and forward pump beam, dependence of PC reflectivity on the backward pump power and forward pump power, and transmittance as a function of time is considered.

12.3 Experimental Configuration

The ray diagram of the phase conjugate wave generation by degenerate four-wave mixing is shown in Fig. 12.2. The probe beam E_3 and the forward-pump beam E_1 interfere in the non-linear material

and create a periodic interference pattern that modulates the physical properties of the non-linear medium. The resulting grating wave vector amplitude is $k = 2\pi/\Lambda$. The fringe period (Λ) can be determined by the well-known formula $\Lambda = \lambda/2\sin(\theta/2)$, where λ is the laser wavelength, and $\pm\theta$ is the forward-pump and probe beam incident angles with respect to the normal to the non-linear medium. The backward-pump beam E_2 is then diffracted under Bragg conditions by the dynamic volume hologram and generates a backward conjugate wavefront whose complex amplitude can be written as E_4.

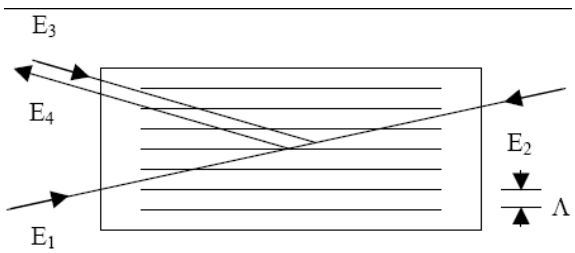

Figure 12.2 Ray diagram of phase conjugate wave generation by degenerate four-wave mixing

The schematic diagram of the phase conjugation experiment is shown in Fig. 12.3. A He-Ne laser (20 mW) beam at 633 nm was divided into three beams, two counter-propagating pump beams E_1 and E_2, namely forward-pump and backward-pump beams respectively and a probe beam E_3 form the DFWM configuration. The spot size of each of these three unfocused beams at the non-linear medium was 1.20 mm in diameter. The constant power ratio of the probe beam (E_3), forward-pump beam (E_1) and backward-pump beam (E_2) used in this work was $\approx 1:10:10$. The angle between the probe beam and the forward-pump beam was 8°. The sample was exposed simultaneously to all these three beams. The optical path lengths of all the three beams were made equal, so that they were coherent at the sample. The phase conjugate wave retraces the path in the opposite direction to that of the probe beam E_3 and was detected with the help of a photodetector and processed by a power meter and data recorder system. The experimental setup was mounted on a vibration isolation table to avoid the destruction of the laser-induced gratings formed in the DASPB dye-doped polymer matrix due to mechanical disturbances.

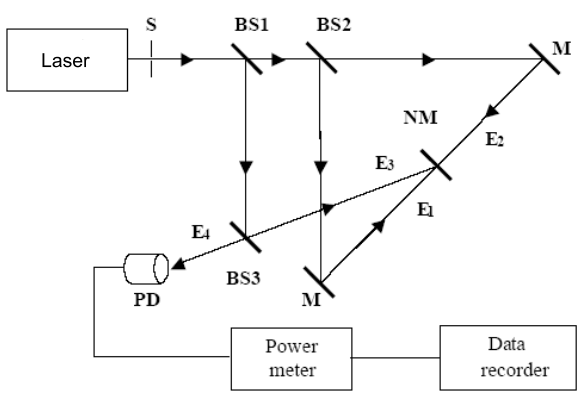

Figure 12.3 Experimental setup for observation of PC wave. S: Shutter; BS1, BS3: Beam splitters; M: Mirror; NM: Non-linear medium; PD: Photo-detector

12.4 Material

One design strategy proposed recently by Albota et al,[3] dealt with molecules based on benzene ring as π-center which is attached symmetrically by either electron–donor (D) or electron–acceptor (A) through various lengths of conjugated connectors; $D-\pi-D$ or $A-\pi-A$. They concluded that σ is increased by increasing the length of conjugation; change with the D/A strength and the extent of symmetric intramolecular charge-transfer (CT) from the D ends to the π-center or vice versa, meaning that symmetric charge redistribution effectively occurs upon excitation of such symmetric molecules.

A similar approach was made in designing molecules by Reinhardt and his coworkers[20] dealing with benzene ring as the π-center which is symmetrically coupled with two electron acceptors ($A-\pi-A$) or asymmetrically with D and A ($D-\pi-A$), respectively. There is no clear effect of structural symmetry on σ values, although increasing conjugation length of π-centers brings about a significant improvement of the value. This seems to suggest that there must be more crucial molecular factors other than structural symmetry involved. In this study, dye molecule as 4-[4-(Dimethylamino)styryl]-1- docosyl pyridinium bromide (DASPB) with π center is used.

12.5 Preparation of Dye-doped Film

Commercially available DASPB (Aldrich Chemical Co.) is purified by recrystallization twice with spectrograde ethanol and by vacuum sublimation. The purity is determined spectroscopically. Purified chloroform is used as the solvent. To prepare the film, polymethyl methacrylate – metacrylic acid was used as polymer matrix. The thin films of DASPB doped in PMMA-MA is prepared using hot press technique. Thin films of variable thickness are obtained between two glass slides. Film thickness of 0.3 mm was prepared with two different dopant concentrations of d_o = 0.001 M and 0.002 M respectively.

12.6 Results and Discussion

12.6.1 Linear optical properties of DASPB

The molecular structure of DASPB is shown in Fig. 12.4. A charge-transfer in between the aromatic moiety (electron donor) and bromine unit (electron acceptor) can be proposed to explain the large χ^3 value measured using Z-scan technique[2]. The linear absorption spectrum of DASPB in chloroform is measured on a VARIAN Cary UV-vis-IR recording spectrophotometer using quartz cuvette with one cm path length as well as doping it in polymethyl methacrylate methacrylic acid (PMMA-MA) film. Figure 12.5 shows the linear absorption spectrum of a DASPB in PMMA-MA with solute concentration of d_0 = 0.001 M. The spectral curve has shown that there is a strong absorption band with peak absorption located at 478 nm with a bandwidth of 100 nm, a medium absorption peaked at 270 nm with a bandwidth of 80 nm and no linear absorption is observed in the entire spectral range of 580 to 2000 nm except IR absorption between 1200 nm to 1600 nm. Styryl dyes are particularly preferred because they have a strong two-photon absorption with a cross-section that is significantly greater than commercial dyes, such as Rhodamine, stilbene and coumarin dyes. The dyes also exhibit intense emission at a wavelength ranging from about 300 to about 680 nm

when excited by laser radiation having a wavelength of from about 660 nm to about 1300 nm. The observation of very strong frequency upconverted fluorescence emission and the subsequent quantitative measurement of the intensity dependence on the near infrared laser excitation proved it to be a two-photon absorption process.

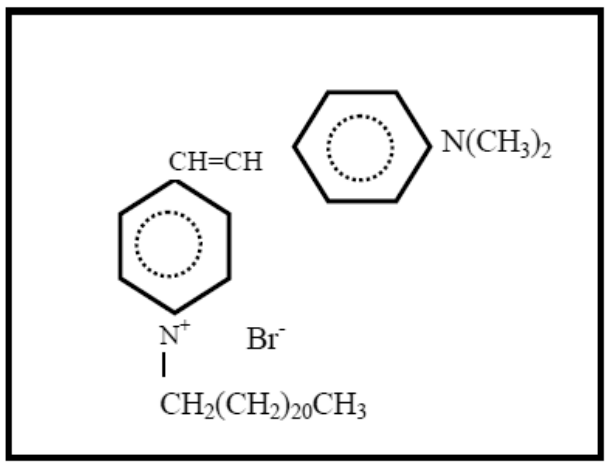

Figure 12.4 Molecular structure of DASPB

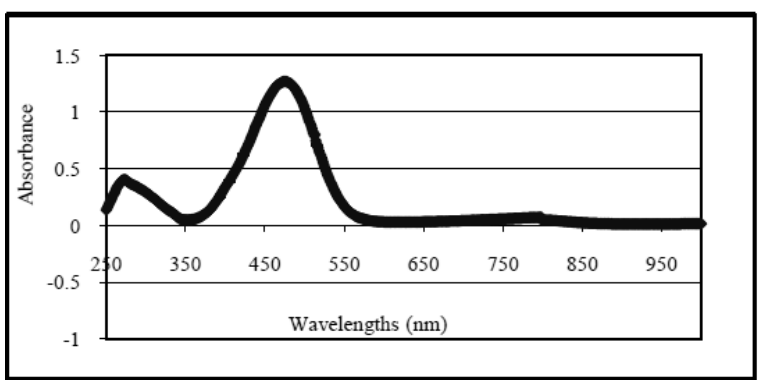

Figure 12.5 Linear absorption spectrum of DASPB in PMMA-MA matrix

12.6.2 Single and two photon florescence property of DASPB

The single photon fluorescence spectrum of the sample is measured for a 1 cm path DASPB in chloroform with the solute concentration of 0.001 mol/L using a spectral fluophotometer (Rf 50000U from Schmadza) with the spectral resolution of 1 nm. The peak wavelength of the single-photon induced fluorescence was 610 nm with a bandwidth of 60 nm (Fig. 12.6). Figure 12.7 corresponds to single photon fluorescence when DASPB is excited at 532 nm using second harmonic of an Nd:YAG laser beam.

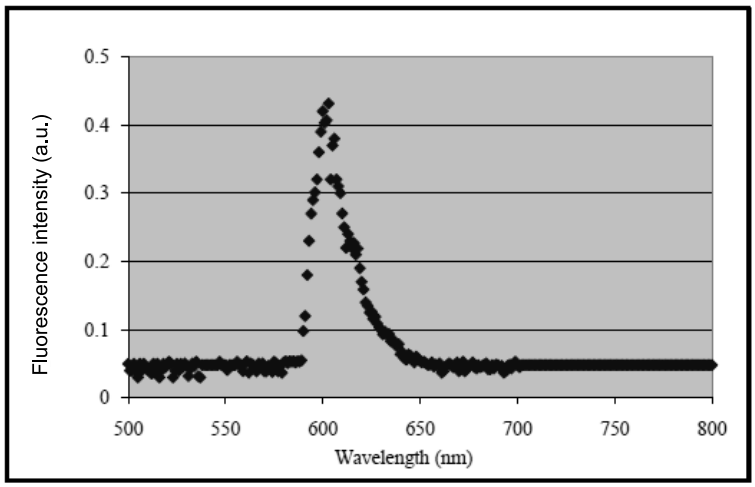

Figure 12.6 Ground state fluorescence spectrum

From the absorption spectrum of DASPB, we can see that there is no linear absorption in the entire spectral range from 580 nm to 1800 nm, except the fact that IR radiation between 1,200 nm to 1,600 nm is strongly absorbed by DSAPB solution. It has been observed that this dye shows quite strong frequency upconverted fluorescence when exposed to near IR and IR laser beam above 700 nm. This suggests that a very strong TPA process may occur inside the sample. The TPA induced emission spectrum of 0.001 M DASPB doped in PMMA-MA polymer matrix excited with 1064 nm laser beam is shown in Fig. 12.8. In the measurement of the upconversion efficiencies, VIS cutting filters were used to cut transmitted pump energy. Comparing Fig. 12.8 with Fig. 12.7, we can see that the TPA induced emission spectrum of DASPB with much higher concentration has a red-shift as compared to that in the much lower concentration single photon absorption study. This can be explained by re-absorption of dye material[28].

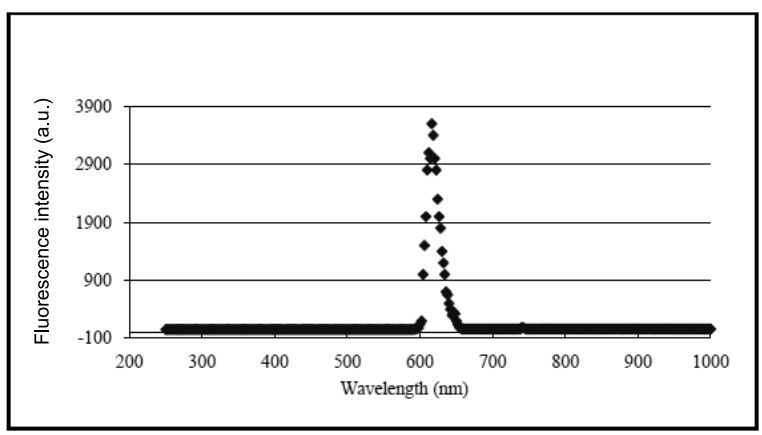

Figure 12.7 One photon induced fluorescence at 532 nm irradiation

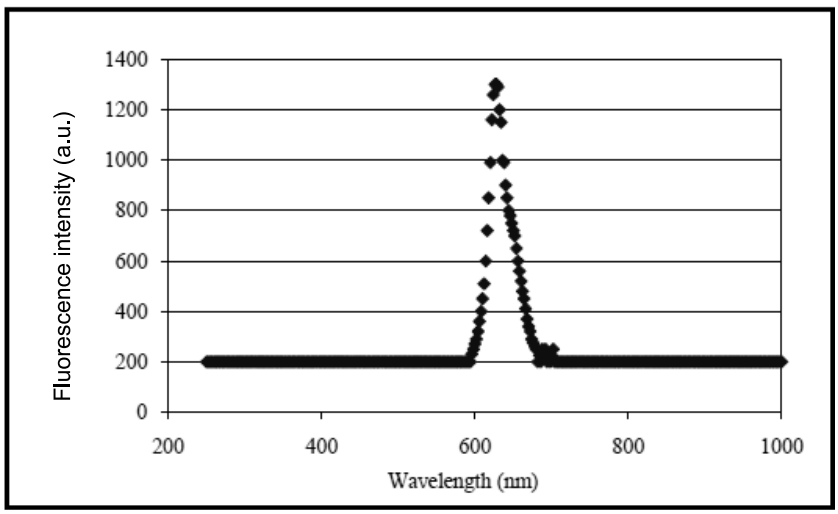

Figure 12.8 Two-photon induced emission spectrum of DASPB at 1.06 μm irradiation

12.6.3 Degenerate four-wave mixing property of DASPB

We consider a three-level system as an energy level diagram of the DASPB dye in PMMA–PA polymer matrix. In this system, S_0 and S_1 are the ground and excited singlet states, respectively, and level T_1 is the triplet state. Absorption of a photon by DASPB results in transition of the DASPB to the first excited singlet state ($S_0 \rightarrow S_1$). If the singlet-to-triplet cross-over is considerable, the dye molecules will switch over to the triplet state ($S_1 \rightarrow T_1$), where they will remain for a relatively longer time as the triplet-to-singlet transition is inhibited, and, consequently, the molecules will not be available for further absorption from the ground state. This will result in a saturation of absorption if the triplet lifetime is long enough. Thus, in the medium, the absorption becomes a function of intensity. Therefore, when the two write beams interfere, the intensity pattern modulates the complex refractive index, which results in the formation of a grating[21]. The probe beam E_3 and the forward-pump beam E_1 interfere in the non-linear material and create a periodic interference pattern that modulates the physical properties of the non-linear medium. The resulting grating wave vector amplitude is $k = 2\pi/\Lambda$. The resultant complex volume hologram is due to a spatial distribution of the refractive index (Kerr-like media), or of the absorption (saturable absorbers or two photon absorption), or of the gain when the conjugator is the laser medium itself. The second anti-parallel pump (backward-pump) beam E_2 is then diffracted under Bragg conditions by the dynamic volume hologram; following the classical formalism of holography, it generates a backward conjugate wavefront whose complex amplitude can be written as $E_4 = E_3^* E_1 E_2$. It is named as the conjugate image beam in holography. Since this geometry involves waves $E_1 - E_4$, which are simultaneously present in the medium, it is known as four-wave mixing. The phase conjugate reflectivity (R_{pc}) is defined as the ratio of the amplitude of the PC wave to the probe beam amplitude [Geethakrishnan T. and Palanisamy P. K., (2005b)].

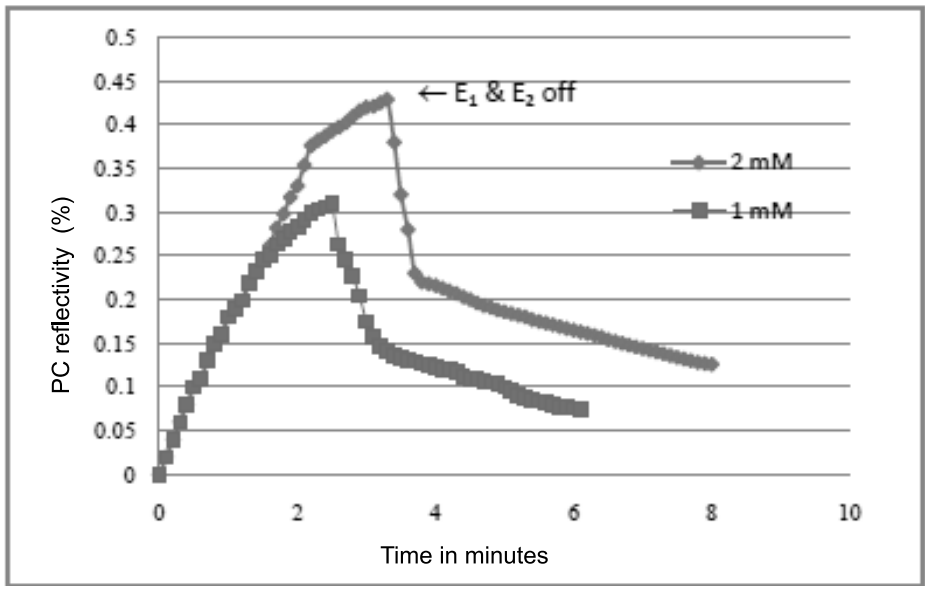

Figure 12.9 PC signal versus recording time for 0.001bM and 0.002 M concentrations

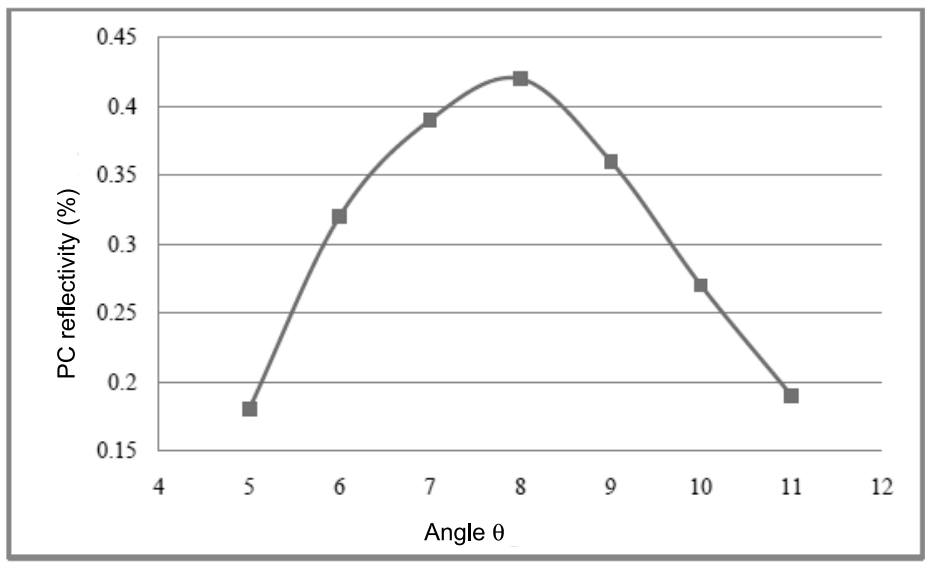

Figure 12.10 PC reflectivity as a function of angle between the probe and the forward pump beams

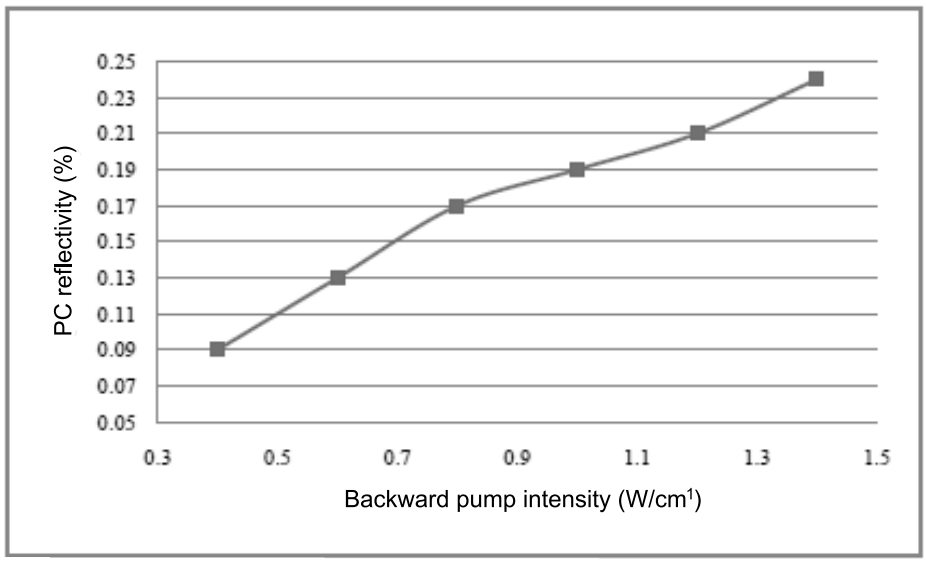

Figure 12.11 Dependence of PC reflectivity on backward pump intensity

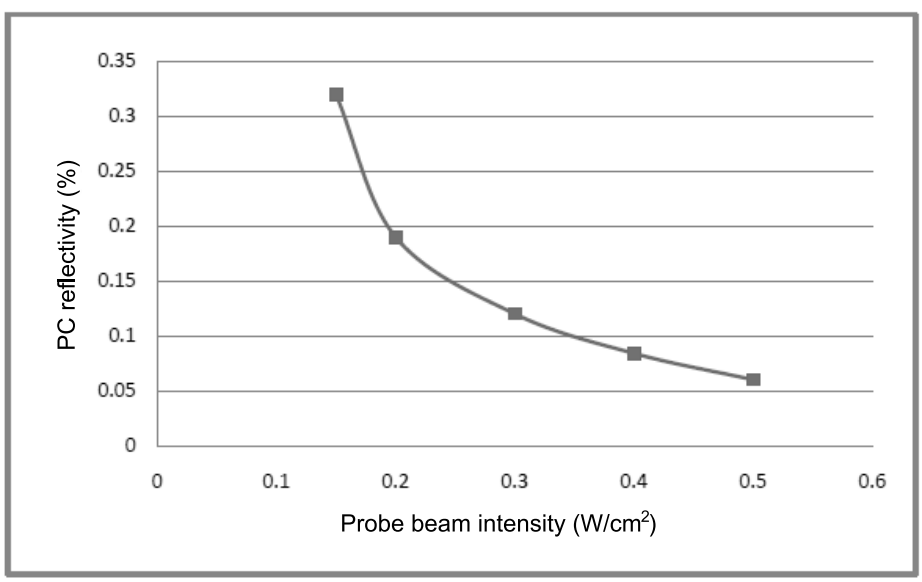

Figure 12.12 Conjugate reflectivity as a function of probe beam intensity

Organic dyes doped in polymer matrix have the capability of generating a phase conjugate wave by not only DFWM but also holographic process[9]. To distinguish the phase conjugate wave generated by DFWM from that by the holographic process, the transient

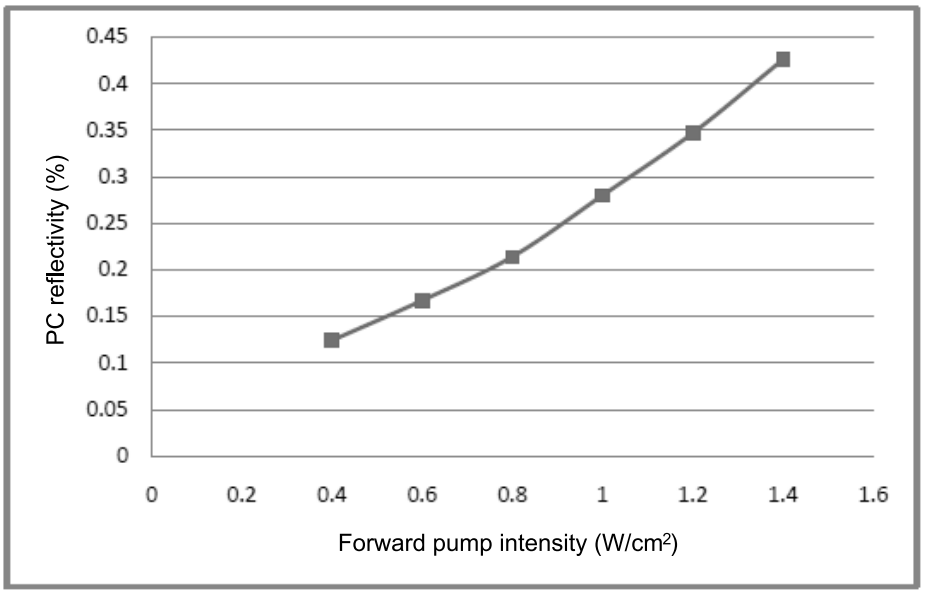

Figure 12.13 Dependence of PC reflectivity on forward pump power

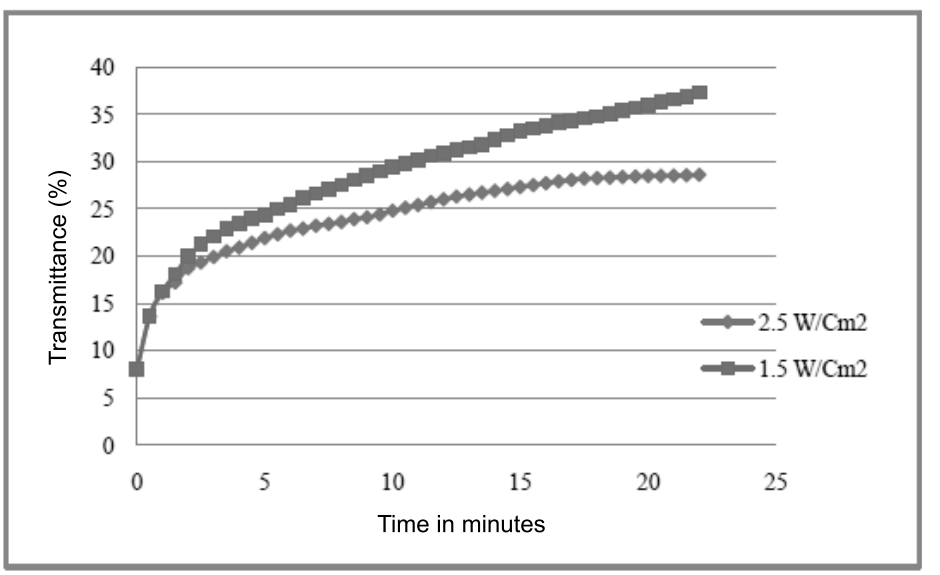

Figure 12.14 Transmittance as a function of time

behavior of the PC signal was studied. For this, the DASPB dye doped in PMMA–PA polymer matrix was first illuminated with three waves E_1, E_2 and E_3 for a specified duration, and afterwards, E_1 and E_3 were successively turned off, so that only E_2 was incident on the dye film. Here, the duration for which all the three waves are incident on the dye film is called as the DFWM duration.

Figure 12.9 shows the measured phase conjugate signal as a function of time. The initial rise to a peak within a few minutes is due to DFWM and holographic processes; the sudden drop in the intensity of the PC signal after shutting off both the write beams E_1 and E_3 indicates the contribution from the fast DFWM process. Due to the holographic process, the PC signal is present even after E_1 and E_3 are shut off, and it decays rather slowly. If the phase conjugate wave was generated only by DFWM, the lack of only one of the three beams E_1, E_2 and E_3 would have stopped generation of the phase-conjugate wave. Therefore, it is inferred that the rapidly decaying component corresponds to the phase conjugate wave which is generated by the DFWM. On the other hand, if spatially modulated information formed by E_1 and E_3 can be recorded in the DASPB dye in the PMMA–PA polymer film, the phase conjugate wave can still be generated when E_2 tries to read this stored information, during the lifetime of the holographic grating.

The PC signal measurements are taken by varying the parameters which influence the PC signal during the DFWM process. Figure 12.9 shows the PC signal versus the time for dye concentration of 0.001 M and 0.002 M doped polymer films. PC intensity rises linearly to a maximum and then starts decreasing. The phase grating formed is transient. To get maximum reflectivities, it is necessary that there be a perfect overlap of the probe and the pump beams in the non-linear medium. Figure 12.10 shows the PC reflectivity as a function of recording angle between the forward pump and probe beam. It seems from the figure that, as the angle between the probe beam and the forward pump beam increases, the PC reflectivity first increases and then decreases. This may be because as the angle increases, the probe beam becomes elliptical and only a fraction of its area falls within the interaction region. Because of two-wave coupling, the maximum PC reflectivity is achieved when the angle is 8 degrees. The effect of the backward pump beam power on the PC reflectivity by keeping the power of the forward pump and probe beams constant and varying the backward pump beam is shown in Fig. 12.11.

Figure 12.12 shows the influence of the input probe beam intensity on the conjugate beam reflectivity. A maximum reflectivity value of 0.42% is observed for probe beam intensity at 1.5 W/cm^2, and further increase in probe beam intensity resulted in decreasing in PC reflectivity. Similar observations have been reported in other kinds of material doped with organic dyes[19]. Figure 12.13 shows the variation of reflectivity for different power of forward pump beam. The PC reflectivity increases linearly with the power of the forward pump beam. There are two main processes which must be considered in the discussion of the origin of OPC in dye doped PMMA–PA films: (1) the formation of thermal grating and (2) third order non-linear optical processes. The DASPB dye doped film illuminated with 632 nm radiation of variable intensity and the transmittance of the sample is measured simultaneously by using a photodetector. If the effect observed in our experiments is of purely thermal nature, bleaching of the sample film should have been observed. The results obtained for the sample are shown in Fig. 12.14. It is clearly demonstrated that the transmission of the sample increases with time. The experiment described above indicates that third order non-linear processes like two photon absorption is mainly responsible for OPC in the sample under study.

12.7 Conclusion

To summarize, low-intensity optical phase-conjugation is observed in DASPB dye in PMMA–PA polymer matrix using a degenerate four-wave mixing setup, employing 633 nm light radiation from a He-Ne laser. The mechanism of phase conjugate wave generation associated with this dye-doped

system is discussed. The phase conjugate signal is found to have contributions from the DFWM and the holographic processes. The maximum phase conjugate beam reflectivity observed in these dye films is about 0.42%. The maximum PC reflectivity is achieved when the angle between the probe and the forward pump beam is 8 degrees. The effects of dye concentration, intensity of backward, forward pump and interbeam angle between probe and forward pump beam on phase conjugation reflectivity are also studied. PC signal first increases with time and then decreases. PC reflectivity is also increased by increasing the intensity of the backward and forward pump beam.

The polarization and intensity profile are verified to be preserved in the conjugate signal. The predominant phase conjugation signal is attributed to the fact that saturable absorption and two photon induced the florescence property of the dye molecules. Since the DASPB dye in PMMA–PA polymer film is used at 633 nm, this may be suitable for low-power semiconductor lasers in the red wavelength region. Thus, DASPB dye in PMMA–PA polymer matrix may be a promising material for real-time double-exposure phase conjugate interferometry.

Bibliography

1. R. L. Abrams and R. C. Lind. 1978. 'Degenerate four-wave mixing in absorbing media.' *Optics Letters* 2, 4: 94–96.
2. S. Aithal, P. S. Aithal, and N. G. Bhat. 2011. 'Optical non-linearity of dye-doped polymer film using Z-scan technique.' *Proceedings of Second International Conference on Photonics IEEEXplore*, ISBN 978-1-61284-265-3, 62–66.
3. M. Albota, D. Beljonne, J. W. Perry, G. Subramanium and C. Xu. 1998. 'Design of organic molecules with large two-photon absorption cross sections.' *Science* 281: 1653–1656.
4. R. W. Boyd. 1992. *Non-linear Optics*, New York, NY, USA: Academic Press.
5. R. Y. Choie, T. H. Barnes, W. J. Sandle, A. D. Woolhouse and I. T. Mc Kinnie. 2000. 'Observation of a thermal phase-grating contribution to diffraction in erythrosin-doped gelatin films.' *Opt. Commun*. 186, 13: 4350.
6. H. Eichler, G. Salje and H. Stahl. 1973. 'Thermal diffusion measurements using spatially periodic temperature distributions induced by laser light.' *Journal of Applied Physics* 44, 12: 5383–5388.
7. H. J. Eichler and O. Mehl. 2001. 'Phase conjugate mirrors.' *J. Non-linear Optical Physics Mater*. 10: 43–52.
8. R. A. Fisher. 1983. *Optical Phase Conjugation*, New York, NY, USA: Academic Press.
9. H. Fujiwara and K. Nakagawa. 1985. 'Transient phase conjugation by degenerate four-wave mixing in saturable dyes.' *Opt. Commun*. 55: 386–390.
10. T. Geethakrishnan and P. K. Palanisamy. 2005. 'Generation of phase-conjugate wave in acid blue 7 dye-doped gelatin film.' *Current Science* 89, 11: 1894–1898.
11. T. Geethakrishnan and P. K. Palanisamy. 2006a. 'Optical phase-conjugation in erioglaucine dye-doped thin film.' *Pramana Journal of Physics* 66, 2: 473–78.
12. T. Geethakrishnan and P. K. Palanisamy. 2006b. 'Degenerate fourwave mixing experiments in methyl green dye-doped gelatin film.' *Optik*. 117, 6: 282–86.
13. G. S. He, J. D. Bhawalkar, C. F. Zhao and P. N. Prasad. 1995. 'Optical limiting effect in a two-photon absorption dye doped solid matrix.' *Appl. Phys. Lett*. 67: 2433–2435.

14. R. W. Hellwarth. 1977. 'Generation of time-reversed wave fronts by non-linear refraction.' *J. Opt. Soc. Am.* 67: 1–3.

15. J. P. Huignard and A. Brignon. 2004. *Overview of Phase Conjugation, Phase Conjugate Laser Optics*. Edited by A. Brignon and J. P. Huignard. ISBN 0-471-43957-6, 1–17 John Wiley & Sons, Inc. New Jersey.

16. M. A. Kramer, W. R. Tompkin and R. W. Boyd. 1986. 'Non-linear optical interactions in fluorescein doped boric acid glass.' *Physical Review A*. 34, 3: 2026–2031.

17. M. S. Malcuit, R. W. Boyd, L. W. Hillman, J. Krasinski and C. R. Stroud. 1984. 'Saturation and inverse-saturation absorption line shapes in alexandrite.' *J. Opt. Soc. Am. B.* 1: 73–75

18. A. Miniewicz, S. Bartkiewicz, J. Sworakowski, J. A. Giacometti and M. M. Costa. 1998. 'On optical phase conjugation in polystyrene films containing the azobenzene dye Disperse Red 1.' *Pure and Applied Optics* 7, 4: 709–721.

19. B. R. Reddy, P. Venkateswarlu and M. C. George. 1991. 'Laser induced gratings in a styryl due.' *Opt. Commun*. 84, 5–6: 334–38.

20. B. A. Reinhardt, L. L. Brott, S. J. Clarson, R. Kannan and A. G. Dillard. 1997. 'The design and synthesis of new organic molecules with large two photon absorption cross sections for optical limiting applications.' *Mater. Res. Soc. Sympo. Proc*. 479: 3–8.

21. A. T. Reghunath, C. K. Subramanian, P. S. Narayanan and M. R. Sajan. 1992. 'Optical phase conjugation in methylene blue films.' *Appl. Opt*. 31: 4905–4906.

22. M. Samoc, A. Samoc, B. L. Davies, H. Reish and U. Scherf. 1998. 'Saturable absorption in poly(indenofluorene): a picketfence polymer.' *Opt. Lett*. 23: 1295–1297.

23. A. E. Siegman. 1986. *Lasers* 207, University Science, California: Mill Valley.

24. Y. Silberberg and I. Bar-Joseph. 1981a. 'Transient effects in degenerate four-wave mixing in saturable absorbers.' *IEEE Journal of Quantum Electronics* 17, 9: 1967–1970.

25. Y. Silberberg and I. Bar-Joseph. 1981b. 'Low power phase conjugation in thin films of saturable absorbers.' *Opt. Commun*. 39, 4: 265–268.

26. L. Solymar, D. J. Webb and A. Grunnet-Jepsen. 1996. *The Physics and Applications of Photorefractive Materials*, Clarendon: Oxford.

27. H. Tanaka, A. Horikoshi, H. Fujiwara and K. Nakagawa. 2002. 'Phase conjugation in saturable absorbing dye films by degenerate four-wave mixing and holographic processes using nanosecond pulse and CW lasers.' *Optical Review* 9, 3: 106–111.

28. C. Wang, Y. Ren, Z. Shao, X. Zhao, G. Zhou, D. Wang, Q. Fang and M. Jiang. 2001. 'Optical properties of new two photon absorbing material HMASPS.' *Non-linear Optics* 28: 1–13.

29. A. Yariv. 1978. 'Phase conjugate optics and real-time holography.' *IEEE J Quantum Electron QE* 14, 9: 650–660.